Stem Cell Reports
Article

ISSCR

OPEN ACCESS

Cryopreservation Maintains Functionality of Human iPSC Dopamine Neurons and Rescues Parkinsonian Phenotypes In Vivo

Dustin R. Wakeman,[1,5,*] Benjamin M. Hiller,[1] David J. Marmion,[1] Christopher W. McMahon,[2] Grant T. Corbett,[1,6] Kile P. Mangan,[2] Junyi Ma,[2] Lauren E. Little,[2] Zhong Xie,[3] Tamara Perez-Rosello,[3] Jaime N. Guzman,[3] D. James Surmeier,[3] and Jeffrey H. Kordower[1,4,*]

[1]Department of Neurological Sciences, Rush University Medical Center, Chicago, IL 60612, USA
[2]Cellular Dynamics International: A Fujifilm Company, Madison, WI 53711, USA
[3]Department of Physiology, Feinberg School of Medicine, Northwestern University, Chicago, IL 60611, USA
[4]The Van Andel Institute, Grand Rapids, MI 49503, USA
[5]Present address: RxGen, Inc., Hamden, CT 06517, USA
[6]Present address: Laboratory for Neurodegenerative Research, Ann Romney Center for Neurologic Diseases, Brigham and Women's Hospital and Harvard Medical School, Boston, MA 02115, USA
*Correspondence: dwakeman@rx-gen.com (D.R.W.), jkordowe@rush.edu (J.H.K.)
http://dx.doi.org/10.1016/j.stemcr.2017.04.033

SUMMARY

A major challenge for clinical application of pluripotent stem cell therapy for Parkinson's disease (PD) is large-scale manufacturing and cryopreservation of neurons that can be efficiently prepared with minimal manipulation. To address this obstacle, midbrain dopamine neurons were derived from human induced pluripotent stem cells (iPSC-mDA) and cryopreserved in large production lots for biochemical and transplantation studies. Cryopreserved, post-mitotic iPSC-mDA neurons retained high viability with gene, protein, and electrophysiological signatures consistent with midbrain floor-plate lineage. To test therapeutic efficacy, cryopreserved iPSC-mDA neurons were transplanted without subculturing into the 6-OHDA-lesioned rat and MPTP-lesioned non-human-primate models of PD. Grafted neurons retained midbrain lineage with extensive fiber innervation in both rodents and monkeys. Behavioral assessment in 6-OHDA-lesioned rats demonstrated significant reversal in functional deficits up to 6 months post transplantation with reinnervation of the host striatum and no aberrant growth, supporting the translational development of pluripotent cell-based therapies in PD.

INTRODUCTION

Parkinson's disease (PD) is a debilitating neurodegenerative disorder afflicting more than 6.3 million individuals worldwide with a staggering 1.5 million patients suffering in the United States alone. More than 55,000 new PD patients are diagnosed each year in the United States, and this number is on the rise with the increasingly aged population.

In PD, degeneration of dopaminergic neurons in the substantia nigra (SN) provides an excellent opportunity for targeted cell-replacement therapy. Evidence from xenografts in rodent and non-human primate models of PD support pre-clinical feasibility (Olanow et al., 1996); however, human clinical trials grafting fetal dopamine neurons have been met with variable results. Several groups described positive long-term outcome measures in small cohorts of PD patients in open-label trials (Barker et al., 2015). However, conflicting reports indicated no consistent long-term reversal in functional deficits associated with transplants in PD patients when assessed in a double-blind fashion (Freed et al., 2001; Olanow et al., 2003). Furthermore, a subset of patients experienced serious side effects including graft-induced dyskinesias. A variety of explanations have been put forth as to the cause of these unforeseen adverse events, including cell-preparation technique, heterogeneous cell composition, and hot spots of innervation (Wakeman et al., 2011).

Pluripotent stem cells are a promising renewable alternative source of dopaminergic neurons and may provide a solution to many of the problems of neural transplantation for PD. Perhaps most importantly, the ability to generate relatively homogeneous populations of lineage-defined neurons in large quantities alleviates the laborious and ethically charged task of sourcing fetal tissue to treat such a large number of PD patients. Recently, several studies demonstrated that pluripotent stem cells can be differentiated into midbrain dopamine neurons, functionally innervate, and reverse behavioral deficits in animal models of PD (Kriks et al., 2011; Kirkeby et al., 2012; Xi et al., 2012; Morizane et al., 2013; Grealish et al., 2015; Hallett et al., 2015; Steinbeck et al., 2015; Chen et al., 2016). In addition, iPSC-mDA neurons offer a number of advantages compared with fetal neurons, including indefinite expandability and immunological matching to the patient, thus eliminating the need for long-term immunosuppression. For these reasons, iPSC-mDA neurons are an extremely promising alternative cellular substrate for transplantation.

For cell-replacement therapy to be a practical option, the process by which cells are derived, reprogrammed,

procured by the clinical site, and grafted needs to be made as simple as possible. Indeed, the generation of a deliverable product that is easily formulated with minimal manipulation is a major challenge for clinical translation of any cell-based therapeutic. From a regulatory perspective, a hurdle for cell therapy in PD remains the significant level of quality control and assurance involved in reliably and efficiently generating a well-defined, production-scale, good manufacturing practice-compliant therapeutic that is capable of being delivered to a large number of patients. Manufacturing a viable frozen product is especially cumbersome for neurons derived from human embryonic stem cells (ESCs) and induced pluripotent stem cells (iPSCs). From a practical and neurosurgical perspective, an ideal cell-based product should be easily and quickly prepared with minimal manipulation at the surgical site to reduce the possibility of human error. Additionally the product should have a long shelf-life and still retain all functional properties. Cryopreservation allows a therapeutic cell product to be easily shipped around the world, drastically increasing availability of the treatment to a large patient pool without need for highly skilled cell-culture technicians or extensive additional quality control and assurance measures. Therefore, cryopreservation of iPSC-mDA neurons that (1) retain their full functional profile, (2) possess high post-thaw viability, and (3) can be prepared without additional subculturing represents a major advancement toward clinical intervention.

A potent methodology was recently developed to generate a highly enriched population of floor-plate-derived midbrain lineage ESC-mDA and iPSC-mDA neurons sufficient to treat the large PD patient population (Kriks et al., 2011). Cellular Dynamics International made a critical translational advancement by developing a methodology to efficiently cryopreserve "footprint-free" post-mitotic iPSC-mDA neurons with high post-thaw viability. To our knowledge, no other technique exists that can reproducibly and efficiently generate a large-scale, clinically relevant, functionally active population of transplantable dopaminergic neurons from pluripotent iPSCs.

While our group has shown considerable therapeutic promise using human ESC-mDA neurons in rodent and non-human primate PD models (Kriks et al., 2011; Wakeman et al., 2014), additional progress needs to be made for iPSC-mDA neurons to reach the clinic. Major points of focus include the ability to thaw cryopreserved cells with good viability and function, as well as a differentiation process that ensures the safety of the cell preparation. Demonstrating functional efficacy and structural correlates of this innovative therapy using clinically applicable cryopreserved iPSC-mDA neurons will allow us to advance pluripotent cell therapy through essential pre-clinical steps toward human clinical trials.

RESULTS

iPSC-mDA Neuron mRNA and Protein Expression Support a Midbrain Lineage Dopaminergic Phenotype

Sixteen different validated production lots of cryopreserved iPSC-mDA neurons were thawed (three vials per lot) and viability was determined. Post-thaw survival averaged 70.0% (±SD 5.3%) live cells across 16 lots (Figure S1A), indicating good post-thaw viability and validating the cryopreservation process across multiple production lots. To determine developmental lineage identity, we thawed cryopreserved iPSC-mDA neurons and control iPSC-derived forebrain neurons (iPSC-FB) and assayed them by qPCR for expression of several dopaminergic, developmental, and neuronal subtype genetic markers. iPSC-mDA neurons had a gene expression profile similar to that of the human SN (Figure 1A). The transcription factors *FOXA2*, *EN1*, *OTX2*, and *LMX1A* were all highly expressed above background levels, indicating a midbrain floor-plate phenotype. Forebrain regional markers such as *FOXG1* or other neuronal subtypes (characterized by *DBH*, *VGlut1*, *CHAT*, or *OLIG2* expression) were expressed poorly or below background levels (Figure 1A). In addition, iPSC-mDA neurons expressed mRNA levels for the dopaminergic markers *TH*, *NURR1*, *GIRK2*, *PTX3*, *DRD2*, *VMAT2*, and *AADC* similar to that of the human SN (Figure 1A), demonstrating that cryopreserved iPSC-mDA neurons retain their mature dopaminergic phenotype after being thawed. Furthermore, at day 17 of differentiation, iPSC-mDA progenitors highly expressed rostrocaudal ventral mesencephalic associated genes *EN1*, *SPRY1*, *PAX8*, *CNPY1*, and *ETV5* with minimal expression of forebrain and hindbrain lineage genes *FOXG1*, *HOXA2*, and *PAX6* (Figure S1B) (Kee et al., 2017), the combination of which were recently reported to be positively associated with dopamine neuron graft yield in vivo (Kirkeby et al., 2017).

Next, we assayed the cryopreserved iPSC-mDA neurons for midbrain lineage dopamine neuron protein markers at various time points. Immunocytochemistry at 7 days post thaw showed that iPSC-mDA neurons exhibited a characteristic neuronal morphology with highly branched processes extending from a large central soma (Figure 1B), and expressed the neuronal protein MAP2 (Figure 1C). In addition, they expressed the midbrain floor-plate marker FOXA2 and roof-plate marker LMX1 with a high percentage of co-localization (91% of total cell population) (Figure 1D), a key characteristic of midbrain dopamine neurons. At 14 days post thaw, iPSC-mDA neurons co-expressed FOXA2 and TH (tyrosine hydroxylase) (Figure 1E)

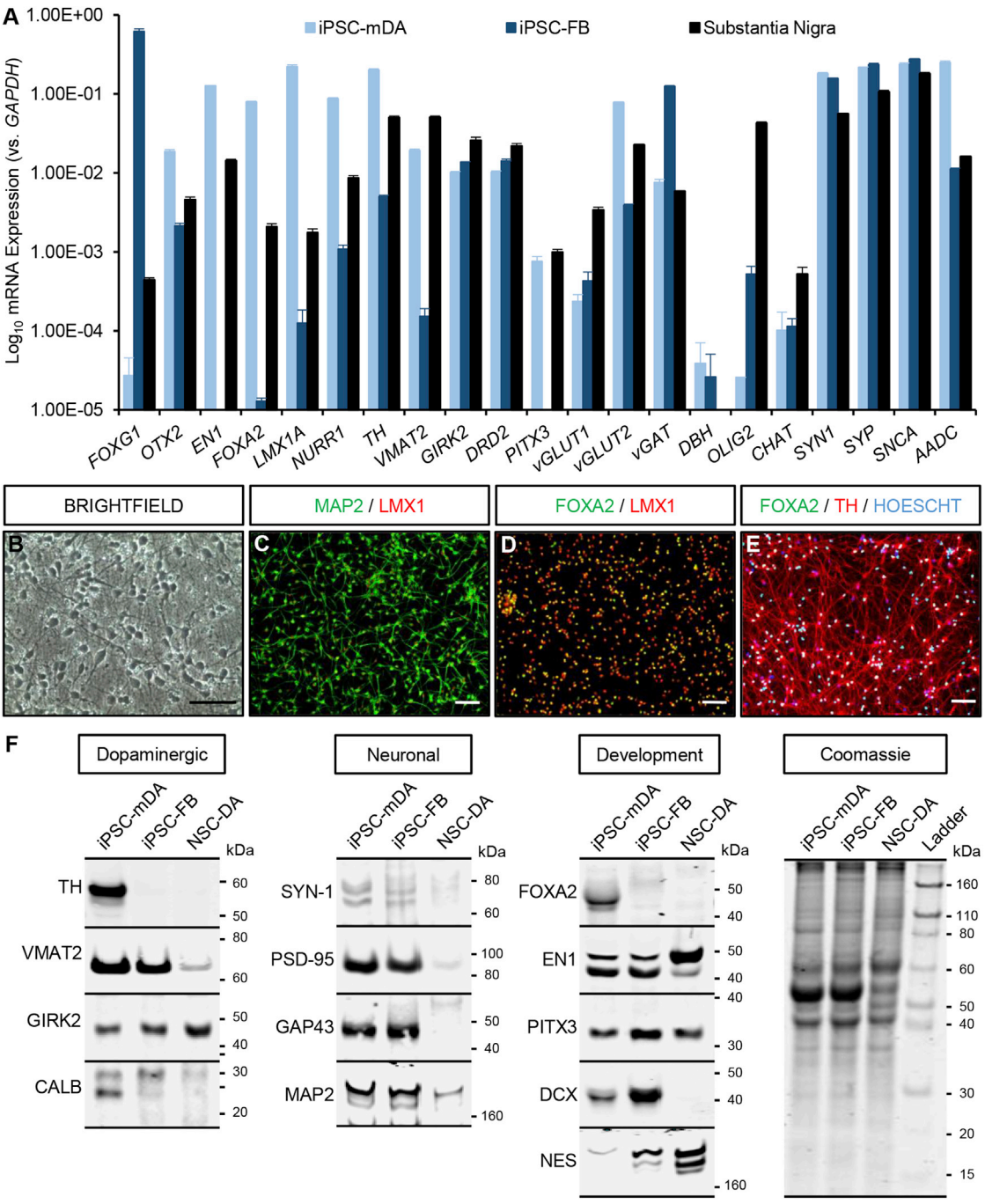

Figure 1. Characterization of Human iPSC-mDA Neurons In Vitro

(A) qPCR comparing mRNA expression of human iPSC-mDA neurons with human SN and human iPSC-FB neurons post thaw (PT) relative to GAPDH (n = 3 independent experiments). Data graphed as average ± SEM. Values $<10^{-4}$ were considered background.

(B–E) Immunocytochemistry of iPSC-mDA neurons at 7 days (B, C, D) or 14 days (E) demonstrating mDA lineage. Scale bars, 100 μm.

(F) Western blots of lysates prepared from iPSC-mDA neurons and controls (iPSC-FB, NSC-DA) confirm a mature dopaminergic lineage profile.

(72.3% of total cells by flow cytometry), with high expression of MAP2 (97.0% of total cells by flow cytometry) and relatively no Nestin (1.4% of total cells by flow cytometry) (Figures S1C and S1D). In addition, Ki-67, a marker for dividing cells, was expressed in ≤0.1% of the thawed cells over a 14-day time course (Figure S2A). Likewise, ≤0.1% of

iPSC-mDA neurons incorporated 5-ethynyl-2′-deoxyuridine into replicating DNA, compared with 93.6% of dividing pluripotent iPSCs (Figure S2B). Together, these data demonstrate that the vast majority of iPSC-mDA neurons are post-mitotic without significant outgrowth of dividing cells at the time of cryopreservation.

To further establish the midbrain dopaminergic neuron identity, we cultured cryopreserved iPSC-mDA neurons in vitro for 28 days and then analyzed them by western blot for expression of neuronal, dopaminergic, and developmental proteins. Analyses confirmed a protein expression profile consistent with the mature midbrain dopaminergic lineage compared with control iPSC-FB neurons or human fetal cortical neural stem cells cultured in iPSC-mDA neuron medium (NSC-DA). iPSC-mDA neurons highly expressed floor-plate lineage proteins FOXA2, EN1, and PITX3 as well as the A9-subtype midbrain dopamine neuron lineage associated proteins TH, VMAT2, and GIRK2 (Figure 1F). The A10-subtype dopamine neuron marker CALB was also present, indicating that multiple midbrain dopamine neuron sublineages were likely present in the cultures (Figure 1F). Furthermore, proteins involved in neuronal maturation and synapse development (SYN1, PSD-95, MAP2, and GAP43) were expressed in iPSC-mDA neurons with relatively low expression of the immature neuron and neural stem cell protein markers (DCX and NES) compared with controls (iPSC-FB or NSC-DA) (Figure 1F). Together, these results indicate that cryopreserved iPSC-mDA neurons can be reliably thawed, cultured long-term, and maintain a floor-plate midbrain dopaminergic neuron lineage expression profile similar to that of the human SN.

iPSC-mDA Neurons Release Dopamine with Functional Electrophysiological Properties In Vitro

Given that the cryopreserved iPSC-mDA neurons retained mRNA and protein expression profiles consistent with midbrain lineage dopamine neurons, we next analyzed their functional output. iPSC-mDA neurons and control iPSC-FB neurons were cultured in vitro for 14 days and then assayed for dopamine secretion by ELISA. Only iPSC-mDA neurons secreted dopamine into the medium, which increased when depolarized with KCl (Figure S2C). As anticipated, iPSC-FB control neurons, which are primarily a mixture of GABAergic and glutamatergic neurons, did not secrete a detectable amount of dopamine (Figure S2C).

To determine the physiological phenotype of iPSC-mDA neurons, we performed a battery of in vitro electrophysiological recordings. A key characteristic of DA neurons in the SN is slow, autonomous pacemaking. At 25°C, voltage-clamp recordings revealed that most (6/10) iPSC-mDA neurons were pacemaking at a low rate (mean firing frequency range: 0.2–4.1 Hz; n = 6) and averaged mean firing frequency of 2.1 ± 0.7 Hz (n = 6) (Figures 2A and 2B). Whole-cell current clamp recordings (n = 3) also showed irregular pacemaking activity (Figure 2C) with a somewhat depolarized firing threshold (−31.10 ± 1.7 mV), long duration action potential (AP) (11.4 ± 0.3 ms), and a prominent afterhyperpolarization (AHP) (15.4 ± 2.7 mV) (Figures 2C and 2D). As expected, the Na^+ and K^+ ion channels underlying this activity responded in a dose-dependent manner to the channel blockers tetrodotoxin and tetraethylammonium, respectively (Figures 2E and 2F). Furthermore, excitatory post-synaptic currents were present at 7 days post thaw (Figure 2G).

We next investigated the connectivity and response of iPSC-mDA neurons to several dopaminergic pharmacological agents. iPSC-mDA neurons cultured on multi-electrode array (MEA) plates displayed synchronous, network-wide bursts at 14 days post thaw that became more synchronous following administration of apomorphine (Figures 2H and 2I). In addition, mean firing rates (MFR) and synchronization levels were positively correlated with gabazine concentration ($p < 0.05$), suggesting that iPSC-mDA neurons develop appropriate network connections and electrophysiological behaviors (Figure 2J). Dopamine pharmacology also displayed dose-dependent increases ($p < 0.05$) in network synchronization but interestingly did not significantly alter MFR across concentrations or pharmacology (Figure 2J), suggesting that dopamine receptor activation alters synaptic connectivity without changing network excitability. Together, the data indicate that cryopreserved iPSC-mDA neurons exhibit appropriate functional electrical firing properties with characteristic ion-channel responses.

Cryopreserved iPSC-mDA Neurons Engraft into the Intact Rodent Brain

Given the in vitro data, we next asked whether freshly thawed iPSC-mDA neurons could survive and function after transplantation into animal models of PD. To mimic the ideal neurosurgical scenario, we thawed functionally validated, cryopreserved cell preparations of iPSC-mDA neurons (identical to those employed in the in vitro western blot, immunocytochemistry, and electrophysiology experiments) and prepared the iPSC-mDA neurons for injection without additional subculturing.

As proof of principle, we first transplanted freshly prepared iPSC-mDA neurons bilaterally into the striatum or unilaterally into the SN of intact, immunosuppressed, non-lesioned adult Sprague-Dawley rats to determine whether they could survive without any additional subculturing. iPSC-mDA neurons were thawed and prepared for transplantation with an average post-thaw viability of 76.5% ± 0.32% as quantified by trypan blue staining just

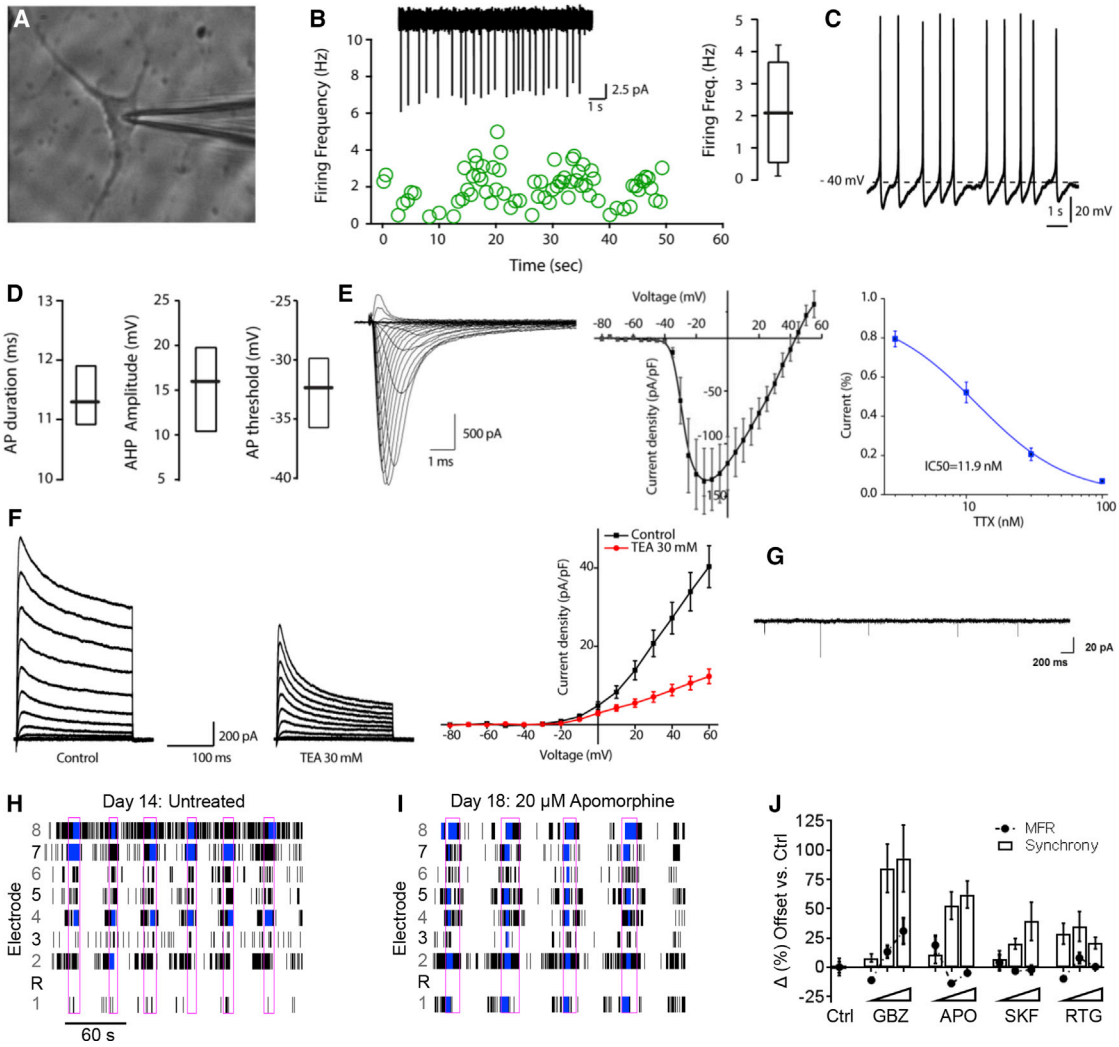

Figure 2. Electrophysiological Characterization of Human iPSC-mDA Neurons

(A) Representative micrograph depicting iPSC neuron and patch electrode.

(B) iPSC-mDA neurons showed irregular spontaneous pacemaking activity at 8 weeks. Time course of firing frequency changes during 1 min of recording on cell-attached patch clamp (inset). Right: box plot of averaged firing frequency (n = 6).

(C) Representative example of spontaneous pacemaker waveform in whole-cell patch clamp.

(D) Summary of action potential (AP) basic properties.

(E) In iPSC-mDA neurons 21 days post thaw: Left: sodium current traces before tetrodotoxin (TTX) application. Middle: current-voltage curve of sodium current. Right: dose-response curve for TTX inhibition of sodium channels.

(F) Potassium current traces before (left) and after (middle) tetraethylammonium (TEA) application. Right: current-voltage curve of potassium current before and after TEA application.

(G) Excitatory post-synaptic currents were recorded in iPSC-mDA neurons 7 days post thaw.

(H) iPSC-mDA neurons cultured onto MEA plates develop synchronized, bursting cultures. Raster plots display synchronized bursts (pink boxes) occurring across all electrodes with Poisson bursts (blue tick-marks) occurring on individual channels.

(I) The same culture presented in (H) after apomorphine treatment shows increased synchronization.

(J) Mean firing rate (MFR) and the synchrony index for cultures treated with increasing concentrations of gabazine (GBZ), apomorphine (APO), the D_1-selective agonist SKF83822 (SKF), and the $D_{3/2}$-selective agonist rotigotine (RTG).

Data in (E), (F), and (J) represent mean ± SD (n = 3 independent experiments).

prior to surgical injection. Rats were euthanized 2 weeks (striatal graft) or 6 weeks (SN graft) post transplantation and assessed histologically to determine cell survival and phenotype. iPSC-mDA neurons transplanted into both the striatum and the SN displayed robust graft survival of human cytoplasm-immunoreactive (huCyto-ir) and human neural cell adhesion molecule-immunoreactive (huNCAM-ir) cells (Figures S3A, S3B, and S3K). Striatal grafts exhibited huNCAM-ir fiber outgrowth extending from the body of the graft into host tissue at 2 weeks post transplant (Figures S3B and S3G). Furthermore, co-localization of FOXA2-ir/TH-ir/huNuclei-ir grafted neurons innervating host striatum demonstrated maintenance of the midbrain dopaminergic lineage in grafted neurons (Figures S3C–S3F). The vast majority of huNuclei-ir cells co-localized with FOXA2, and many FOXA2-ir/huNuclei-ir cells were also TH-ir. The size and density of grafts stained for huNuclei confirmed that transplanted iPSC-mDA neurons were not migratory and remained tightly spaced within the zone of engraftment (Figure S3H). Stereological counts of huNuclei-ir cells revealed average survival of 90,387 ± 17,354 (21.07%) of the total cryopreserved iPSC-mDA neurons that were initially injected. In adjacent, level-matched sections, no proliferative Ki-67-ir cells were found in any grafts (Figures S3I and S3J).

After 6 weeks in vivo, iPSC-mDA neuron grafts in the SN projected huNCAM-ir fibers caudally from the graft body located in the SN, along the nigrostriatal path, toward the striatum (Figure S3K). In addition, the TH-ir cell bodies contained in grafts at 6 weeks post transplant were considerably more mature in their morphology than the 2-week striatal grafts (Figures S3L and S3M). SN TH-ir neurons typically had a large, angular soma with extensive arborizations (Figure S3N) that innervated the host striatum (Figures S3O and S3P), indicating that the neurons continued to develop over time.

iPSC-mDA Neurons Survive, Innervate, and Maintain Midbrain Dopaminergic Phenotype in 6-OHDA-Lesioned PD Rats

Upon establishing excellent survival of cryopreserved iPSC-mDA neurons in the intact rodent brain, we sought to determine whether cryopreserved iPSC-mDA neurons could ameliorate functional deficits in the 6-hydroxydopamine (6-OHDA) lesioned rat model of PD. Adult Sprague-Dawley rats were unilaterally lesioned with 6-OHDA into the right medial forebrain bundle (MFB) to create a stable dopaminergic lesion. Only animals that exhibited sustained rotational asymmetry following d-amphetamine injection were used to assess functional output. At 12 to 14 weeks post lesion, cryopreserved iPSC-mDA neurons (n = 10 rats) or vehicle control (basal medium without growth factor supplements; n = 5 rats) were transplanted into the ipsilateral lesioned striatum of cyclosporine immunosuppressed rats and behaviorally tested for 6 months until euthanasia and histological examination (Figure S4A).

At 6 months post injection, immunosuppressed 6-OHDA-lesioned Sprague-Dawley rats grafted with cryopreserved human iPSC-mDA neurons showed excellent graft survival with extensive innervation of huNCAM-ir fibers throughout the entire engrafted striatum (Figure 3A). Similar to grafts in intact animals, huNuclei-ir cell bodies appeared healthy, with few condensed or blebbing nuclei, and remained within the injection site (Figure 3B). Cells did not migrate extensively into peripheral brain structures; however, iPSC-mDA neurons did spread out within the graft zone compared with 2-week grafts, leading to an increase in graft volume and subsequent reduction in overall density.

Histological analysis demonstrated unilateral ablation of endogenous TH-ir midbrain dopaminergic neurons in the SN and their striatal projections in vehicle control and iPSC-mDA neuron injected rats, anatomically confirming a complete MFB lesion (Figures 3C, 3E, 3F, and S4C), thus validating the stable d-amphetamine rotational asymmetry data. Therefore, evidence of dopaminergic terminals within the lesioned hemisphere would be a direct result of grafted dopaminergic neurons innervating the host striatum and not a result of host circuitry restoration or compensation. Indeed, transplanted human iPSC-mDA neurons were TH-ir, innervated the entire striatum (Figures 3D and S4B), and co-localized with huNCAM-ir fibers throughout the grafted hemisphere (Figures 3G–3I). Optical density measurements from the injected striatum confirmed a statistically significant increase in TH-ir fibers within the iPSC-mDA neuron grafted striatum compared with vehicle controls (Figure S4D). In addition, at 6 months post transplant, grafted TH-ir neurons exhibited highly developed, mature dopaminergic morphology with extensively arborized axons that expansively innervated host parenchyma (Figures 3J and S4E). Triple immunofluorescence staining for TH, FOXA2, and huNuclei showed co-expression of all three markers in grafted iPSC-mDA neurons (Figures 3K–3N), confirming maintenance of the midbrain dopaminergic lineage following long-term engraftment.

In PD patients, there is a preferential degeneration of A9-subtype dopamine neurons located in the SN compared with the relatively preserved neighboring A10-subtype dopamine neurons of the ventral tegmental area. Given that western blot data indicated the presence of both A9-subtype (which express GIRK2) and A10-subtype (which express Calbindin) dopaminergic neurons in our cell population, we next analyzed grafted tissue for these lineage-defining markers to determine graft composition. As expected, the majority of mature TH-ir grafted cells were also GIRK2-ir (Figures 3O–3R); however, there were

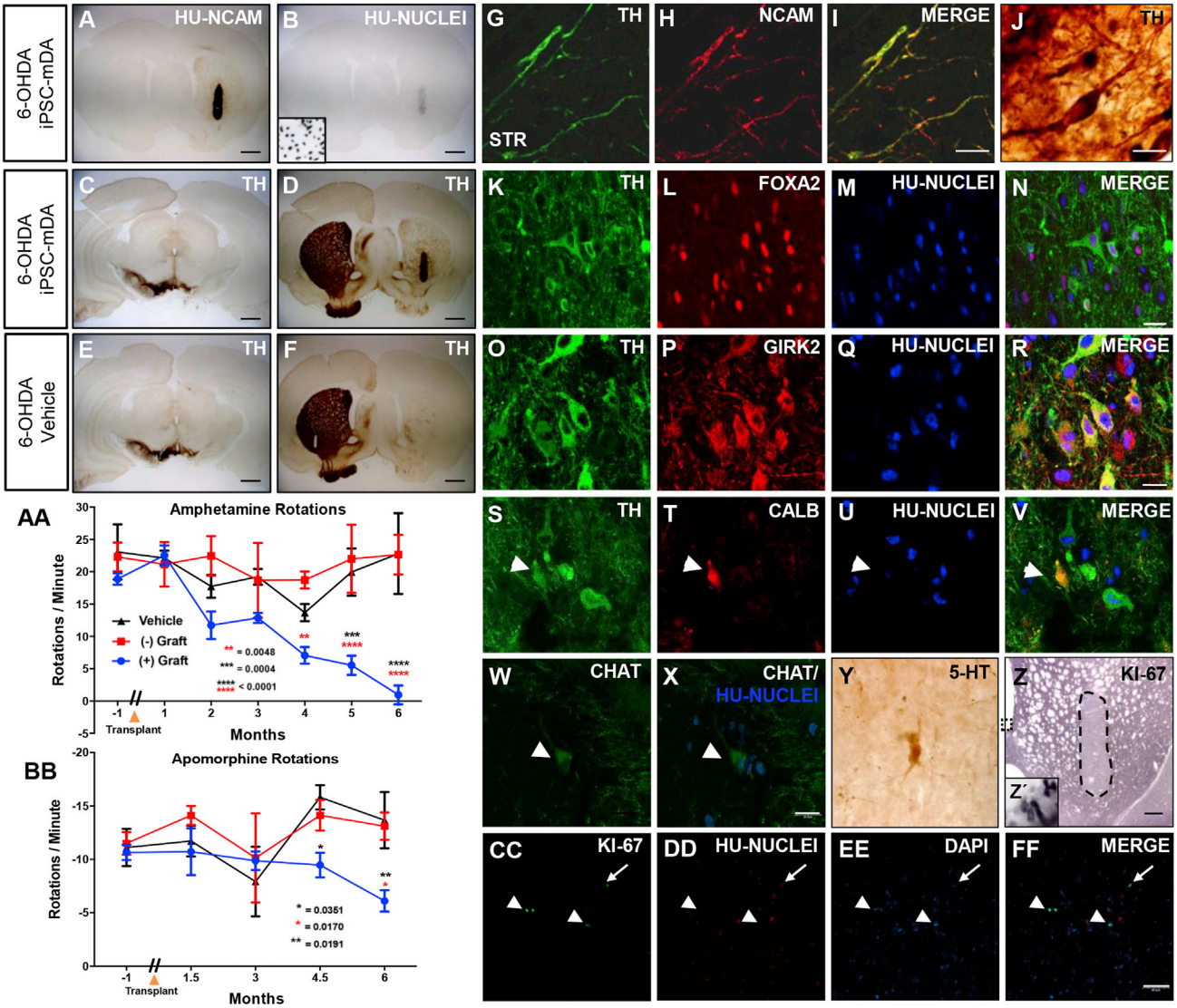

Figure 3. iPSC-mDA Neurons Rescue Motor Deficits in 6-OHDA Rats

(A and B) Extensive innervation of (A) huNCAM-ir fibers and (B) biodistribution of huNuclei-ir iPSC-mDA neurons.

(C–F) Striatal dopaminergic innervation of iPSC-mDA neurons (C and D) compared with vehicle control (E and F).

(G–I) Human NCAM-ir/TH-ir fibers in ventral striatum are graft derived.

(J) Mature grafted TH-ir neurons.

(K–V) Grafted TH-ir neurons retain midbrain dopaminergic phenotype (K–N) and are predominantly of the A9 lineage (O–R) versus A10 lineage (S–V). Arrowheads demarcate double-labeled cells.

(W–Y) Only a few cholinergic (CHAT-ir/huNuclei-ir; W and X) or serotonergic (5-HT-ir; Y) cells were found in the grafts.

(Z and CC–FF) Analysis of proliferative Ki-67-ir cells within the (Z) graft compared with (inset, Z′) the endogenous stem cells of the ventricular layer. Of the few Ki-67-ir cells in the graft, the majority were not huNuclei-ir (arrowheads). Individual Ki-67-ir/huNuclei-ir cells (arrows) were rarely found and never in multiples of two.

(AA and BB) 6-OHDA rats with successful grafts (n = 6, blue line) demonstrated statistically significant reversal in (AA) amphetamine and (BB) apomorphine-induced rotational asymmetry compared with animals with unsuccessful grafts (n = 4, red line) or vehicle controls (n = 5, black line). Negative y axis in (BB) denotes contralateral rotation compared with positive y axis for ipsilateral rotation in (AA). Data graphed as average ± SEM (AA: **p = 0.0048, ***p < 0.0004, ****p < 0.0001; BB: * (black) p = 0.0351, * (red) p = 0.0170, **p = 0.0191). Scale bars, 1 mm (A–F), 10 μm (I), 15 μm (J, R), and 20 μm (N, X).

some mature Calbindin-ir/TH-ir dopamine neurons within the iPSC-mDA neuron grafts at 6 months post transplantation (Figures 3S–3V), confirming the presence of both midbrain dopaminergic neuron subpopulations. In addition, we found a very small number of CHAT-ir/huNuclei-ir (Figures 3W and 3X) and 5-hydroxytryptamine (5-HT)-ir cells within the grafts (Figure 3Y). Overall, these findings indicate that the overwhelming majority of cryopreserved iPSC-mDA neurons maintained a midbrain floor-plate dopaminergic phenotype and continued to mature over time in vivo.

iPSC-mDA Neurons Rescue Motor Deficits in Parkinsonian Rats

Upon histological examination, six of the ten 6-OHDA-lesioned rats that were transplanted with iPSC-mDA neurons contained successful huNCAM-ir/huCyto-ir/huNuclei-ir grafts. We therefore hypothesized that the animals that did not demonstrate successful engraftment, possibly due to lack of sufficient sustained immunosuppression levels, should not recover following injection and would have behavioral deficits similar to those of vehicle-injected control rats. As a result, we divided the ten total grafted animals into two groups, (1) successful graft (n = 6) and (2) unsuccessful graft (n = 4), and analyzed the results for both rotational asymmetry tasks. Critically, animals with successful grafts (n = 6, blue line) demonstrated statistically significant reversal in d-amphetamine- and apomorphine-induced rotational asymmetry compared with animals with unsuccessful grafts (n = 4, red line) or vehicle controls (n = 4, black line), indicating both dopamine release from grafted iPSC-mDA neurons and normalization of D2 receptor activity secondary to innervation, respectively (Figures 3AA and 3BB). Histological confirmation of dopaminergic degeneration in the SN (Figure 3C) suggests that the behavioral improvements in iPSC-mDA grafted rats were a direct result of graft innervation into the host and rescue of dopaminergic transmission and not due to rescue of endogenous midbrain neurons. Of note, results for both rotational asymmetry tasks were statistically significant prior to separating the grafted animals into successful and unsuccessful grafts. This demonstrates the robustness of the effects on these tasks since, in a post hoc analysis, unsuccessful grafts and vehicle controls did not differ from each other ($p > 0.05$). By parsing out the noise of unsuccessful grafts, we were able to determine the actual levels of behavioral recovery induced by successful engraftment.

For patient safety, it is imperative that iPSC-mDA neuron grafts do not proliferate extensively following transplantation. Actively proliferating cells may be an indication of contaminating stem cells that have not exited the cell cycle or the onset of tumorigenesis, either of which could be detrimental if allowed to grow unchecked in PD patients. To this end, we analyzed grafted neurons for Ki-67 as a marker for proliferation in sections level-matched to huNuclei-ir stained sections. Very few sporadic Ki-67-ir human cells were located within the body of the graft (Figures 3Z and 3CC–3FF), but we did not find any histological evidence indicative of proliferative or tumorigenic anatomical structures. In those few cases, only one Ki-67-ir/huNuclei-ir cell was found (Figure 3EE, arrow), and never accompanied by a second cell that might indicate active proliferation. A few endogenous Ki-67-ir microglia that were not huNuclei-ir were found within the graft (Figure 3EE, arrowhead). This finding is critical for establishing pre-clinical safety going forward.

Grafted iPSC-mDA Neurons Display High Survival Rate and Dopaminergic Phenotype

We next performed unbiased stereological counting to quantify the overall survival and dopaminergic composition of grafted iPSC-mDA neurons. In healthy, unlesioned animals, we found an average of 21.07% cell survival. Similarly, in 6-OHDA-lesioned rats that had successful grafts, we found on average 101,580 ± 10,326 huNuclei-ir nuclei (22.57% of total cells injected) within the grafted striatum after 6 months in vivo.

Stereological estimates of grafted TH-ir neurons in the striatum of 6-OHDA-lesioned rats revealed an average of 26,081 ± 2,009 TH-ir grafted cells of dopaminergic phenotype after 6 months (34.49% of total surviving huNuclei-ir cells). However, the overall percentage of huNuclei-ir/TH-ir neurons varied. Perhaps the most striking finding was that the animal with the poorest cell survival (2%; 9,679 huNuclei-ir) had the highest percentage of dopamine neurons (60%; 5,838 TH-ir), and the animal with the highest cell survival (39%; 177,694 huNuclei-ir) had the lowest percentage of dopamine neurons (13%; 22,317 TH-ir). Yet despite this variability, all six successfully grafted rats had complete reversal in d-amphetamine-induced rotations and statistically significant improvement in apomorphine-induced rotational asymmetry.

Grafted iPSC-mDA Neurons Innervate and Mature in the Non-human Primate Striatum

After establishing both initial safety and efficacy in the 6-OHDA rodent model of PD, we next sought to determine how cryopreserved iPSC-mDA neurons would be tolerated in the dopamine-depleted, non-human primate brain as proof of principle for long-term investigational new drug-enabling studies. Injection of the neurotoxin MPTP (1-methyl-4-phenyl-1,2,3,6-tetrahydropyridine) into primates induces degeneration of TH-ir dopaminergic neurons within the SN and denervation of nigrostriatal afferents, resulting in depletion of dopaminergic tone (Kordower et al., 2000, 2006).

We injected human iPSC-mDA neurons into the anterior putamen of mildly symptomatic, immunosuppressed MPTP-treated cynomolgus macaque monkeys and surveyed the brain at both 1 month (n = 3) and 3 months (n = 1) post transplantation. To differentiate between monkey and human cells, we used a human-specific antibody (human cytoplasm; huCyto) that does not cross-react with monkey cells. At 4 weeks post transplantation, cryopreserved human iPSC-mDA neurons survived and projected extensive huCyto-ir fibers into the host striatum (Figures 4A and 4B). By 3 months post transplantation, huCyto-ir cells projected densely arborized fibers innervating into host tissue (Figures 4E and 4J–4L).

Additionally, at 3 months post transplant, huCyto-ir iPSC-mDA grafts injected into the putamen were TH-ir and developed characteristic mature neuronal morphology with robust fiber outgrowth (Figures 4D–4N). Compared with 1 month post grafting, TH-ir iPSC-mDA neuron cell bodies had a more mature morphology with large, arborized, angular soma (Figures 4D and 4I). Inverted images of grafted huCyto-ir neurons demonstrated maturation of human iPSC-mDA neurons at 3 months (Figures 4K and 4L) compared with the relatively immature bipolar morphology seen at 1 month post graft (Figure 4C). Interestingly, following fetal VM transplant clinical trials, the majority of TH-ir cell bodies were found at or near the periphery of the graft, with fewer cells in the central core. This was not observed with these cells. Instead, TH-ir neurons were evenly distributed throughout the body of the graft (Figure 4H). Of note, there are no TH-ir dopamine neuron cell bodies in the striatum; therefore, all TH-ir/HuCyto-ir neurons were unequivocally of donor origin (Figures 4D–4F). Furthermore, many grafted TH-ir neurons retained the midbrain A9-lineage, co-expressing FOXA2 and GIRK2 (Figures 4M and 4N). As with the 6-OHDA rat, we found no evidence of aberrant growth or tumor-like structures in any monkey grafts, indicating initial safety using cryopreserved iPSC-mDA neurons in the best pre-clinical animal model for PD.

DISCUSSION

In the present study, we have shown proof of principle that cryopreserved, post-mitotic iPSC-mDA neurons can be thawed without manipulation, survive, innervate, express dopaminergic markers, and reverse behavioral deficits without tumor formation. Human iPSCs were differentiated into midbrain lineage dopamine neurons and cryopreserved. Substantial supporting data, including biochemical assays for mDA lineage and dopamine secretion as well as electrophysiological parameters, indicated that thawed iPSC-mDA neurons retained phenotypic and functional parameters of the midbrain dopaminergic fate.

We next sought to decipher the long-term retention of intrastriatal iPSC-mDA neuron grafts in animal models of PD, an important step for rationally advancing toward clinical trials. We chose to approach this fundamental question using a simple and rapid cell preparation protocol that would enable most neurosurgeons in a modern surgical suite to effectively deliver this cell-replacement therapy to patients. Cryopreserved iPSC-DA neurons were prepared for injection without additional subculturing and injected into dopamine-depleted rats and monkeys. In 6-OHDA-lesioned rats, grafted neurons with mature neuronal morphology extensively innervated the entire striatum and rescued functional deficits. When injected into dopamine-depleted monkeys, cryopreserved iPSC-mDA neurons retained mature dopaminergic phenotype and innervated host striatum.

Several key results indicated promising initial safety in grafted animals. Of critical importance, we found no evidence for aberrant proliferation at both short-term and long-term time points, consistent with the high purity and mature phenotype of cells cultured in vitro. PD patients are expected to live several decades beyond surgical intervention; therefore, elimination of tumorigenic cells prior to engraftment is of penultimate importance for patient safety.

Biodistribution of cells is an important measure for clinical consideration. When neural progenitor cells are injected into the brain they can be highly migratory, especially through white matter tracts. Here we found little to no migration of cells away from the body of the graft. Rather, over time in the rodent brain, we noticed that transplanted neurons spread slightly and thus occupied a larger volume while reducing their overall cell density. This may be an effect of iPSC-mDA neurons maturing and innervating host brain, remodeling and "making space" for new synaptic connections. The mechanism responsible for grafted neurons remaining within the zone of injection versus the highly migratory behavior of neural precursor cells is unknown and warrants future investigation to determine whether it is cell intrinsic or related to the microenvironment. Regardless of the mechanism, extensive fiber innervation was seen throughout the entire striatum; therefore if cell migration was inhibited, it did not affect the growth of fibers or functional connectivity to the host, as all animals with successful grafts displayed functional recovery. Similar patterns of functional fiber outgrowth with synaptic integration to and from host circuitry have been reported by others using freshly prepared cells (Chen et al., 2016; Grealish et al., 2015; Steinbeck et al., 2015).

Of equal importance will be characterization of the lineage of donor cells that were not TH-ir. A recent report that examined the same iPSC-mDA neurons using single-cell

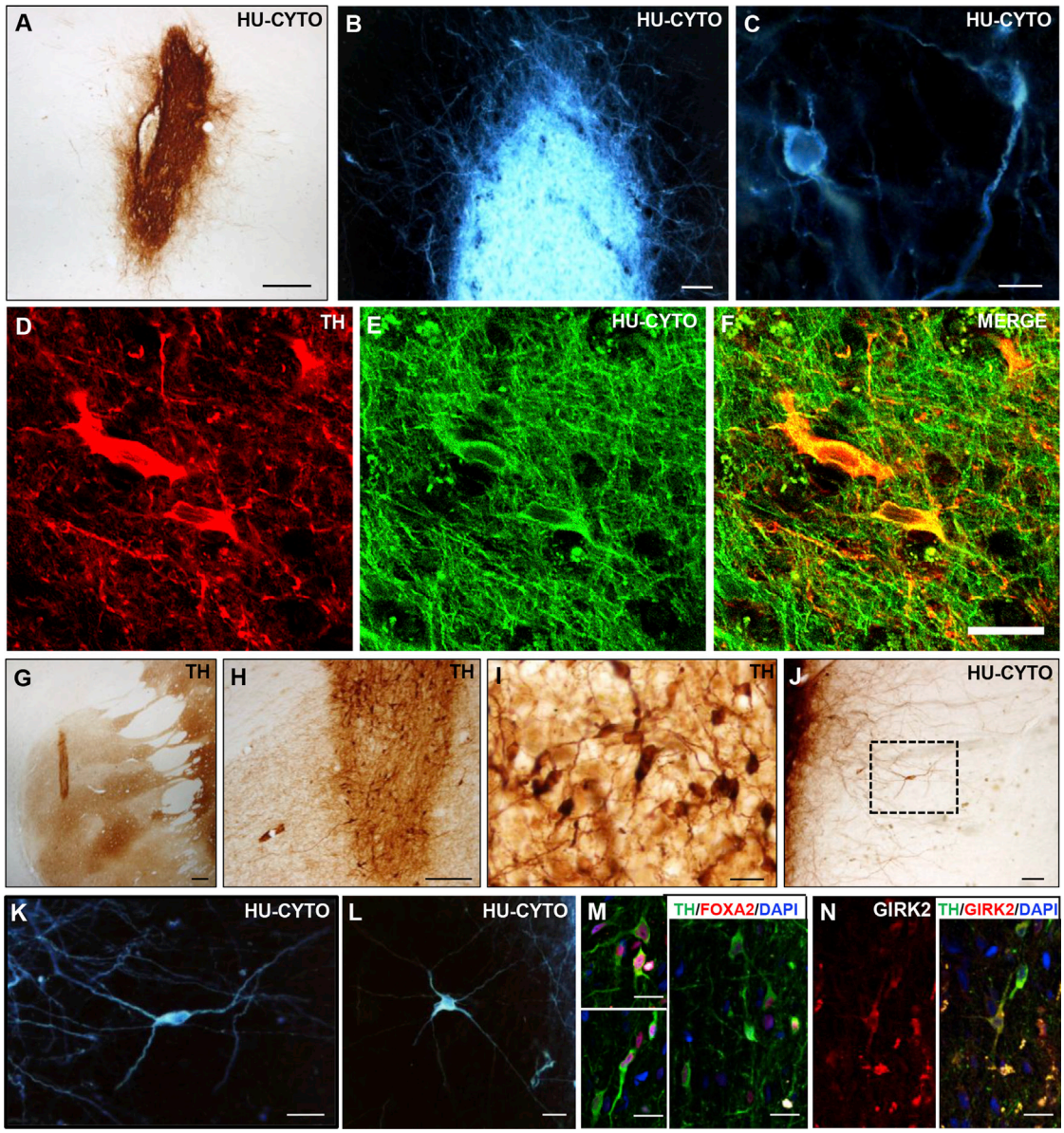

Figure 4. iPSC-mDA Neurons Innervate the Dopamine-Depleted Monkey Brain

(A–C) HuCyto-ir graft of iPSC-mDA neurons in MPTP-lesioned monkey. Higher-magnification inverted images of (B) huCyto-ir fiber innervation and (C) immature bipolar morphology at 1 month post transplant.

(D–I) Grafted iPSC-mDA neurons are TH-ir and HuCyto-ir at 3 months post transplantation into the striatum of MPTP-treated cynomolgus macaques.

(J–L) Grafted huCyto-ir iPSC-mDA cells display mature neuronal morphology. (K and L) Inverted images of the (K) huCyto-ir neuron outlined in (J) and another representative (L) huCyto-ir donor cell demonstrating axonal branching and mature morphology of grafted neurons.

(M and N) iPSC-mDA neurons retain (M) midbrain floor-plate phenotype consistent with (N) A9 dopaminergic lineage.

Scale bars, 500 μm (G), 250 μm (A, H), 25 μm (I, K, L), 50 μm (B, J), and 20 μm (C, F, M).

RNA sequencing suggests that they are dopaminergic progenitors that have not yet matured into TH-ir neurons (La Manno et al., 2016). Those results indicate that the cryopreserved population of cells includes multiple lineages across a developmental continuum with a large proportion sharing expression patterning with authentic human midbrain dopamine neurons, similar to fetal ventral mesencephalon tissue currently being transplanted into

PD patients in Europe. Long-term studies are currently under way to determine whether these cryopreserved iPSC-mDA progenitor subtype cells continue to mature in vivo as their fetal counterpart. In addition, two recent reports identified optimized differentiation techniques and a key genetic signature beyond expression of *FOXA2* and *LMX1A* that appear to improve grafting outcome and dopaminergic maturation in vivo (Kee et al., 2017; Kirkeby et al., 2017). We assayed iPSC-mDA neurons used in this study for the same genes at day 17 of differentiation and found that they were indeed all highly expressed, thus confirming that the cell population in this study are similar to the lineage-purified cells of Kirkeby et al. (2017).

Recent studies indicated that the number of grafted dopamine neurons required to produce functional recovery in 6-OHDA-lesioned rats is relatively low (Grealish et al., 2015). In the present study, we report an average of ~21% cell survival from cryopreserved cells. This fraction is similar to what other groups have reported using freshly prepared, non-cryopreserved cell populations. Similar to previous reports, we found little to no evidence of proliferating cells; therefore, the number of post-mitotic surviving cells accurately represents graft survival and will be critical for calculating clinical dosing.

In the present study, all 6-OHDA-lesioned rats with successful grafts displayed functional improvements, with reversal in both rotational asymmetry behavioral tasks despite variability in overall cell survival and number of TH-ir neurons present within the graft. These results are consistent with previous reports utilizing pluripotent stem cell-derived dopamine neurons in PD rodents (~5,000–18,000 TH-ir neurons) (Kirkeby et al., 2012; Kriks et al., 2011), yet only ~500–1,000 surviving TH-ir dopamine neurons were necessary to induce complete reversal in amphetamine-induced rotations (Grealish et al., 2014). Therefore, extensive graft innervation of even a small percentage of surviving neurons is likely to provide significant therapeutic benefit and should help guide pre-clinical dosing studies. It is important to note that four of the original ten 6-OHDA-lesioned rats did not retain surviving grafts. These animals may not have properly metabolized the cyclosporine immunosuppressant, and thus rejected the xenografts. To follow up this finding, we transplanted 16 immunodeficient rats (RNU-NUDE), using the exact techniques described here, and found graft survival in all 16 NUDE rats (data under review for separate paper), supporting the notion that the four animals in the present study underwent xenograft rejection from inadequate immunosuppression.

A major complication associated with fetal dopamine neuron grafts in clinical trials was the eventual manifestation of graft-induced dyskinesias in a subset of patients (Lane and Winkler, 2012). In some patients, the graft-induced-dyskinesias were sufficiently severe that they required a second brain surgery, deep brain stimulation, to control the sporadic movements. Graft-induced dyskinesias were not predicted as a potential side effect from pre-clinical work grafting fetal dopamine neurons, as they often require several years of growth and innervation before clinical manifestation. Many explanations have been asserted as to the cause for graft-induced dyskinesias; however, it is clear that a concerted effort should be made going forward to address whether pluripotent stem cell-based therapies will also induce such negative side effects.

Empirical evidence from several decades of transplanting fetal dopamine neurons, neural stem cells, or other neural derivatives strongly argues that rescuing behavioral deficits in rodent experimental PD does not always translate to success at ameliorating motor deficits in MPTP-lesioned parkinsonian monkeys. Therefore, it is imperative that pluripotent cell-based therapies are ultimately tested for safety, toxicity, and efficacy in the best model currently available for PD, the MPTP-lesioned monkey (Wakeman et al., 2006). Only a large animal model with a complex brain structure that more accurately mimics the human condition can provide the kind of analytical data necessary to move into human clinical trials. This is particularly important when evaluating the degree of innervation necessary for functional recovery. Being able to time and quantify the degree of innervation in non-human primates will enhance our ability to predict what might be expected following human grafting. That being said, MPTP-induced parkinsonism only accurately models dopamine-related motor symptoms of PD, a small subset of the symptoms experienced in late-stage PD. Therefore, cell-replacement therapy, no matter what the source, likely will not have any significant long-term impact on non-motor features of PD, especially those that affect the autonomic nervous system. Furthermore, slowing the progression of the disease, likely through an intervention that targets the spread and aggregation of toxic α-synuclein species, will also likely be needed. A combination therapy of dopamine cell replacement with modulators of α-synuclein may prove successful to slow both the progression of the disease while simultaneously providing exogenous dopamine through targeted intervention with iPSC-mDA neurons.

Our innovative approach provides solutions to significant obstacles in PD cell-replacement therapy. The findings we report here focus on well-characterized, functionally active, midbrain-specific iPSC-mDA neurons as an alternative patient-matched renewable source for cellular transplantation. We utilized a readily deliverable cryopreserved cell formulation highly amenable to the clinical setting and provide proof of principle for clinical delivery of cryopreserved midbrain iPSC-mDA neurons that are accessible to a large PD patient population. Our results revealed

excellent safety and efficacy in a rodent model of PD using cryopreserved iPSC-mDA neurons, and validate future pre-clinical testing in parkinsonian monkeys. Utilizing easily accessible, frozen stocks of transplantable neurons with no manipulation is a major breakthrough for the field and demonstrates pre-clinical feasibility for clinical application in a variety of neurodegenerative disorders as well as broader implications for application of cryopreserved cell-based therapeutics covering a vast array of regenerative medicine disciplines.

EXPERIMENTAL PROCEDURES

Derivation of iPSC-mDA Neurons

iPSC-mDA neurons were derived from an iPSC line made by Cellular Dynamics International from peripheral blood collected from a consented donor using an episomal, footprint-free technology as previously described (Yu et al., 2009). qPCR was used to verify the loss of reprogramming plasmids and the lack of plasmid integration to the genome. The parental iPSC line was engineered with a construct inserted into the AAVS1 site encoding a neomycin resistance gene driven by the human *Map2* promoter, to select for neuronal cell types. iPSCs were differentiated into midbrain lineage dopamine neurons via floor-plate specification and dopaminergic maturation based on published literature (Kriks et al., 2011), utilizing small-molecule inhibitors of GSK-3 and SMAD signaling, and activation of the Hedgehog signaling pathway. Improved progenitor patterning was obtained by adding all small-molecule inhibitors at the initiation of differentiation and optimizing inhibitor concentrations, as has been described in the literature (Kirkeby et al., 2012; Xi et al., 2012). mDA progenitors were plated in maturation medium (Kriks et al., 2011) and passaged weekly (process days 24 and 31) using Accutase (Innovative Cell Technologies). After additional cell handling and workflow improvements, including negative selection with G418 (Geneticin) to remove non-neuronal cells, a finalized manufacturing protocol with excellent reproducibility was established. mDA neurons were harvested for cryopreservation on process days 33 or 38 by dissociating the cells after incubation with Accutase (37°C, 45 min). Cells were centrifuged and resuspended in cell-culture basal medium for measuring cell viability and counts using a ViCELL XR automated cell counter (Beckman Coulter). Cells were centrifuged again, and the pellet was gently resuspended at 1.25×10^7 cells/mL in ice-cold CryoStor Freeze Media (BioLife Solutions), a serum free, cGMP cryopreservant. The cells were aliquoted at 1 mL/cryovial and cryopreserved with a CryoMed controlled rate freezer (Thermo Fisher Scientific), using a stepwise cooling program to obtain a sample temperature drop of approximately 1°C/min. Upon reaching −60°C, the cooling rate was accelerated to 10°C/min until reaching −100°C, at which point the cryovials were transferred to the vapor phase of a liquid nitrogen tank. The cell-harvesting procedures, timing of cryopreservation, and cryopreservation protocol were optimized to yield post-mitotic iPSC-mDA neurons with high post-thaw viability and plating efficiency. Both in-process and prior to cryopreservation, and then again post thaw, iPSC-mDA neurons demonstrated post-mitotic midbrain neuron purity via flow cytometry analysis ($FOXA2^+$, $LMX1^+$, TH^+, $MAP2^+$, NES^-, $TRA\text{-}1\text{-}81^-$; data not shown for LMX1 and TRA-1-81). In addition, iPSC-mDA neurons exhibited high post-thaw viability with characteristic morphology and neurite outgrowth in vitro. Cryopreserved iPSC-mDA neurons were procured from Cellular Dynamics International and standard iPSC-mDA neurons are sold under the commercial name iCell DopaNeurons.

Research Animals

All animal procedures were performed with Institutional Animal Care and Use Committee approval from Rush University Medical Center and/or Animal Care Committee approval from the University of Illinois at Chicago.

SUPPLEMENTAL INFORMATION

Supplemental Information includes Supplemental Experimental Procedures, four figures, and two tables and can be found with this article online at http://dx.doi.org/10.1016/j.stemcr.2017.04.033.

AUTHOR CONTRIBUTIONS

D.R.W. conceived and designed the study, collected and assembled data, performed data analysis and interpretation, wrote the manuscript, and made final approval of the manuscript. C.W.M. and G.T.C. collected and assembled data, performed data analysis and interpretation, and wrote the manuscript. B.M.H., D.J.M., K.P.M., J.M., L.E.L., Z.X., T.P.-R., J.N.G., and D.J.S. collected and/or assembled data and performed data analysis and interpretation. J.H.K. designed the study, carried out data interpretation, and edited the manuscript.

ACKNOWLEDGMENTS

We thank Clive N. Svendsen for providing the human fetal cortical neural stem cells, Rachel Harker and Scott Muller for exceptional primate husbandry, Cedric Bardy and the Salk Institute for providing the BrainPhys medium used in MEA analysis, Carrie Chavez and Lucas Chase for technical expertise, and Kim Staats for editorial suggestions to the manuscript. This work was supported in part by grants to D.R.W. from Rush University Medical Center: Department of Neurological Sciences and Translational Sciences Consortium, as well as funding from Cellular Dynamics International, Inc. J.H.K. was supported by a center grant from the Parkinson's disease Foundation. This work also was supported by grants from the JPB Foundation and NIH (NS NS047085) to D.J.S. C.W.M., K.P.M., L.E.L., and J.M. are employees at Cellular Dynamics International, Inc.

Received: December 20, 2016
Revised: April 26, 2017
Accepted: April 27, 2017
Published: June 1, 2017

REFERENCES

Barker, R.A., Drouin-Ouellet, J., and Parmar, M. (2015). Cell-based therapies for Parkinson disease—past insights and future potential. Nat. Rev. Neurol. *11*, 492–503.

Chen, Y., Xiong, M., Dong, Y., Haberman, A., Cao, J., Liu, H., Zhou, W., and Zhang, S.C. (2016). Chemical control of grafted human PSC-derived neurons in a mouse model of Parkinson's disease. Cell Stem Cell *18*, 817–826.

Freed, C.R., Greene, P.E., Breeze, R.E., Tsai, W.Y., DuMouchel, W., Kao, R., Dillon, S., Winfield, H., Culver, S., Trojanowski, J.Q., et al. (2001). Transplantation of embryonic dopamine neurons for severe Parkinson's disease. N. Engl. J. Med. *344*, 710–719.

Grealish, S., Diguet, E., Kirkeby, A., Mattsson, B., Heuer, A., Bramoulle, Y., Van Camp, N., Perrier, A.L., Hantraye, P., Bjorklund, A., et al. (2014). Human ESC-derived dopamine neurons show similar preclinical efficacy and potency to fetal neurons when grafted in a rat model of Parkinson's disease. Cell Stem Cell *15*, 653–665.

Grealish, S., Heuer, A., Cardoso, T., Kirkeby, A., Jonsson, M., Johansson, J., Bjorklund, A., Jakobsson, J., and Parmar, M. (2015). Monosynaptic tracing using modified rabies virus reveals early and extensive circuit integration of human embryonic stem cell-derived neurons. Stem Cell Reports *4*, 975–983.

Hallett, P.J., Deleidi, M., Astradsson, A., Smith, G.A., Cooper, O., Osborn, T.M., Sundberg, M., Moore, M.A., Perez-Torres, E., Brownell, A.L., et al. (2015). Successful function of autologous iPSC-derived dopamine neurons following transplantation in a non-human primate model of Parkinson's disease. Cell Stem Cell *16*, 269–274.

Kee, N., Volakakis, N., Kirkeby, A., Dahl, L., Storvall, H., Nolbrant, S., Lahti, L., Björklund, Å.K., Gillberg, L., Joodmardi, E., et al. (2017). Single-cell analysis reveals a close relationship between differentiating dopamine and subthalamic nucleus neuronal lineages. Cell Stem Cell *20*, 29–40.

Kirkeby, A., Grealish, S., Wolf, D.A., Nelander, J., Wood, J., Lundblad, M., Lindvall, O., and Parmar, M. (2012). Generation of regionally specified neural progenitors and functional neurons from human embryonic stem cells under defined conditions. Cell Rep. *1*, 703–714.

Kirkeby, A., Nolbrant, S., Tiklova, K., Heuer, A., Kee, N., Cardoso, T., Ottosson, D.R., Lelos, M.J., Rifes, P., Dunnett, S.B., et al. (2017). Predictive markers guide differentiation to improve graft outcome in clinical translation of hESC-based therapy for Parkinson's disease. Cell Stem Cell *20*, 135–148.

Kordower, J.H., Emborg, M.E., Bloch, J., Ma, S.Y., Chu, Y., Leventhal, L., McBride, J., Chen, E.Y., Palfi, S., Roitberg, B.Z., et al. (2000). Neurodegeneration prevented by lentiviral vector delivery of GDNF in primate models of Parkinson's disease. Science *290*, 767–773.

Kordower, J.H., Herzog, C.D., Dass, B., Bakay, R.A., Stansell, J., 3rd, Gasmi, M., and Bartus, R.T. (2006). Delivery of neurturin by AAV2 (CERE-120)-mediated gene transfer provides structural and functional neuroprotection and neurorestoration in MPTP-treated monkeys. Ann. Neurol. *60*, 706–715.

Kriks, S., Shim, J.W., Piao, J., Ganat, Y.M., Wakeman, D.R., Xie, Z., Carrillo-Reid, L., Auyeung, G., Antonacci, C., Buch, A., et al. (2011). Dopamine neurons derived from human ES cells efficiently engraft in animal models of Parkinson's disease. Nature *480*, 547–551.

La Manno, G., Gyllborg, D., Codeluppi, S., Nishimura, K., Salto, C., Zeisel, A., Borm, L.E., Stott, S.R., Toledo, E.M., Villaescusa, J.C., et al. (2016). Molecular diversity of midbrain development in mouse, human, and stem cells. Cell *167*, 566–580.

Lane, E.L., and Winkler, C. (2012). L-DOPA- and graft-induced dyskinesia following transplantation. Prog. Brain Res. *200*, 143–168.

Morizane, A., Doi, D., Kikuchi, T., Okita, K., Hotta, A., Kawasaki, T., Hayashi, T., Onoe, H., Shiina, T., Yamanaka, S., et al. (2013). Direct comparison of autologous and allogeneic transplantation of iPSC-derived neural cells in the brain of a non-human primate. Stem Cell Reports *1*, 283–292.

Olanow, C.W., Kordower, J.H., and Freeman, T.B. (1996). Fetal nigral transplantation as a therapy for Parkinson's disease. Trends Neurosci. *19*, 102–109.

Olanow, C.W., Goetz, C.G., Kordower, J.H., Stoessl, A.J., Sossi, V., Brin, M.F., Shannon, K.M., Nauert, G.M., Perl, D.P., Godbold, J., et al. (2003). A double-blind controlled trial of bilateral fetal nigral transplantation in Parkinson's disease. Ann. Neurol. *54*, 403–414.

Steinbeck, J.A., Choi, S.J., Mrejeru, A., Ganat, Y., Deisseroth, K., Sulzer, D., Mosharov, E.V., and Studer, L. (2015). Optogenetics enables functional analysis of human embryonic stem cell-derived grafts in a Parkinson's disease model. Nat. Biotechnol. *33*, 204–209.

Wakeman, D.R., Crain, A.M., and Snyder, E.Y. (2006). Large animal models are critical for rationally advancing regenerative therapies. Regen. Med. *1*, 405–413.

Wakeman, D.R., Dodiya, H.B., and Kordower, J.H. (2011). Cell transplantation and gene therapy in Parkinson's disease. Mt. Sinai J. Med. *78*, 126–158.

Wakeman, D.R., Weiss, S., Sladek, J.R., Elsworth, J.D., Bauereis, B., Leranth, C., Hurley, P.J., Roth, R.H., and Redmond, D.E. (2014). Survival and integration of neurons derived from human embryonic stem cells in MPTP-lesioned primates. Cell Transplant. *23*, 981–994.

Xi, J., Liu, Y., Liu, H., Chen, H., Emborg, M.E., and Zhang, S.C. (2012). Specification of midbrain dopamine neurons from primate pluripotent stem cells. Stem Cells *30*, 1655–1663.

Yu, J., Hu, K., Smuga-Otto, K., Tian, S., Stewart, R., Slukvin, I.I., and Thomson, J.A. (2009). Human induced pluripotent stem cells free of vector and transgene sequences. Science *324*, 797–801.